

# UC Berkeley

## UC Berkeley Previously Published Works

**Title**

Variability of Millennial-Scale Trends in the Geomagnetic Axial Dipole

**Permalink**

<https://escholarship.org/uc/item/1qq6c9kq>

**Journal**

Geophysical Research Letters, 46(24)

**ISSN**

0094-8276

**Authors**

Buffett, B  
Davis, W  
Avery, MS

**Publication Date**

2019-12-28

**DOI**

10.1029/2019GL085909

Peer reviewed

# Variability of millennial-scale trends in the geomagnetic axial dipole

B. Buffett<sup>1</sup>, W. Davis<sup>1</sup> and M. S. Avery<sup>1</sup>

<sup>1</sup>Department of Earth & Planetary Science, University of California, Berkeley

## Key Points:

- Statistics of dipole trends depend on the length of the time window.
- A stochastic model reproduces the statistics of paleomagnetic trends.
- Sustaining the historical trend to produce a polarity transition is unlikely.

## Abstract

The historical trend in the axial dipole is sufficient to reverse the field in less than 2 kyr. Assessing the prospect of an imminent polarity reversal depends the probability of sustaining the historical trend for long enough to produce a reversal. We use a stochastic model to predict the variability of trends for arbitrary time windows. Our predictions agree well with the trends computed from paleomagnetic models. Applying these predictions to the historical record shows that an extrapolation of the current trend for next 1 to 2 kyr is highly unlikely. Instead, we compute the trend and time window needed to reverse the field with a specified probability. We find that the dipole could reverse in the next 20 kyr with a probability of 2%.

## 1 Introduction

Observatory data show that the axial dipole moment (ADM) has been decreasing at an average rate of 6% per century since the inception of measurements in 1840 (Gillet et al., 2013). This sharp decline has prompted widespread speculation about an impending polarity reversal (Hulot et al., 2002; De Santis et al., 2013; Laj & Kissel, 2015). Extrapolating the historical rate for the next 1.66 kyr is sufficient to bring the amplitude of the axial dipole to zero, marking the start of the next polarity interval. A relevant question is whether the historical rate will persist for the next 1 to 2 kyr. We frame this question in terms of probabilities of various outcomes. For example, what is the probability of sustaining the current rate over a time interval equal in length to the historical record? This would tell us whether the current trend is unusual. We would also like to know the probability of sustaining this trend over 2 kyr. Extending the record using paleomagnetic observations offers insights, but the message is not always clear. Paleomagnetic intensity measurements support a lower rate of decline over the past 1 kyr (Poletti et al., 2018), but there are several instances in the past 7 kyr when larger trends did not persist for long enough to cause a reversal (Constable & Korte, 2006).

It is reasonable to expect the probability of a given trend to depend on the time window of interest. For example a very long time window is expected to give a trend close to zero when the dipole moment has a well-defined mean value (i.e. the mean converges as the record length increases). Reducing the time interval allows larger slopes to occur, although the expected value of many shorter trends may still be close to zero.

It is helpful to illustrate these ideas using 200-year trends in the dipole field from the CALS10k.2 model (Constable et al., 2016). The time-dependent Gauss coefficient,  $g_1^0(t)$ , is converted to an axial dipole moment,  $x(t)$ , (e.g. Constable, 2007) but we adopt a sign convention that makes the present-day axial dipole moment positive. Trends,  $b$ , are computed by a least-squares fit of  $x(t)$  to

$$x(t) = bt + a \quad (1)$$

over 200-year time intervals. Non-overlapping time intervals are taken to ensure independence in the estimates of  $b$ . A histogram of the resulting 200-year trends is shown in Figure 1. The mean trend is close to zero, whereas the standard deviation is  $\sigma_b = 1.84 \times 10^{22} \text{ A m}^2 \text{ kyr}^{-1}$ . By comparison, the historical trend between 1840 and 2010 is  $4.54 \times 10^{22} \text{ A m}^2 \text{ kyr}^{-1}$  (Gillet et al., 2013), corresponding to  $2.5\sigma_b$  event. While the historical trend is unusual in the light of variability in the CALS10k.2 model, there are times in the last 10 kyr when the amplitude of the slope was as large or larger than the historical trend (see Figure 1). Modifying the calculation to consider 500-year trends reduces the standard deviation to  $\sigma_b = 1.4 \times 10^{22} \text{ A m}^2$ . A hypothetical 500-year decrease at the current historical rate would correspond to a  $3.1\sigma_b$  event. The probability of this outcome would be less than 0.1%, based on a normal distribution.

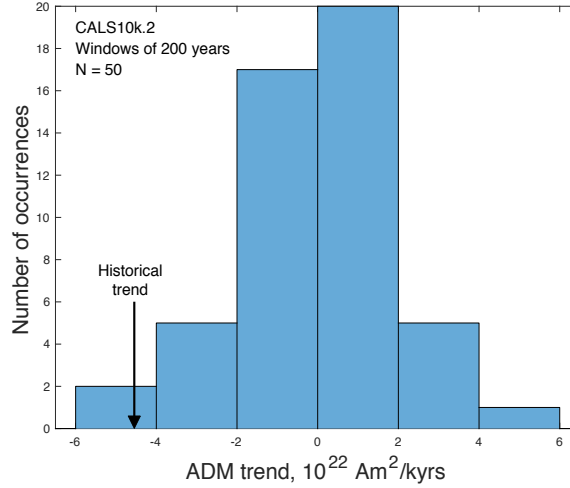


**Figure 1.** Histogram of 200-year trends in the axial dipole moment (ADM) computed from the CALS10k.2 model. Each trend is computed from a non-overlapping time interval (or window length). The mean trend is close to zero, but variations are as large as the historical trend.

Extending the trends in the CALS10k.2 model much beyond 500 years is a challenge because longer windows mean fewer independent estimates of the trend. Similarly, we cannot rely solely on models with temporal variations constrained by marine sedimentary records and ADM amplitudes calibrated by absolute paleointensity records (e.g. Ziegler et al., 2011; Valet et al., 2005) because these models lack sufficient resolution at timescales of several kyr. However, we can use paleomagnetic observations to construct a stochastic model for the geomagnetic axial dipole, and use the theory of stochastic processes to quantify the variability in the trend as a function of window length  $w$ . The theory allows us to focus on the window length of interest, although we can still test our predictions using paleomagnetic observations at window lengths that are amenable to these records.

We find that the probability of maintaining the current rate of decline for the next 2 kyr is implausibly low. This result is consistent with a previous inference based on data assimilation of paleomagnetic observations (Morzfeld et al., 2017). We can also quantify the average trend (and hence the time interval) needed to bring the dipole moment to zero with a specified probability. The model predicts that the dipole moment could vanish over the next 20 kyr with a 2% probability. A remarkably similar prediction was obtained by different means using a solution of the backward Fokker-Planck equation (Buffett & Davis, 2018). We establish these results by first showing how a stochastic model can be used to characterize the variability in the dipole trend as a function of window length.

## 2 Stochastic Model for the Dipole Moment

Fluctuations in the axial dipole moment,  $x(t)$ , are described by a stochastic differential equation

$$dx = v(x)dt + \sqrt{2D(x)} dW_t, \quad (2)$$

where the drift term,  $v(x)$ , describes the deterministic evolution of the dipole moment and the noise (or diffusion) term,  $D(x)$ , defines the amplitude of random variations (Buffett et al., 2014). The time dependence of the random process,  $dW_t$ , represents uncorrelated

**Table 1.** Model parameters and standard deviation (in brackets)

Parameter	Value	Units
$\gamma$	0.1 (0.0033)	kyr <sup>-1</sup>
$\tau_\gamma$	10 (0.34)	kyr
$D$	$0.34 (0.0072) \times 10^{44}$	A <sup>2</sup> m <sup>4</sup> kyr <sup>-1</sup>
$\alpha$	8.56 (1.93)	kyr <sup>-1</sup>
$\tau_\alpha$	0.12 (0.2)	kyr
$\tau_{sed}$	1.75 (0.05)	kyr

(white) noise from a Gaussian distribution with a mean of zero and a variance of  $dt$ . The random term can also be interpreted as an increment in a Wiener process (Van Kampen, 2007). Numerical solutions for the discrete version of (2) are obtained using the Euler-Maruyama scheme (Risken, 1989). Although higher-order approximations exist (e.g. Kloeden & Platen, 2013), this scheme provides adequate pathwise convergence for our requirements.

Models of paleointensity from the past 2 Myr (Ziegler et al., 2011; Valet et al., 2005) suggest that the drift term can be approximated using a linear function

$$v_l(x) = -\gamma(x(t) - x_0) \quad (3)$$

where  $\gamma$  defines the rate of relaxation of the dipole moment toward the stable point  $x_0$ . The timescale for relaxation is  $\tau_\gamma = \gamma^{-1}$ . A modification of (3) was proposed by Buffett and Puranam (2017) to allow for large departures of  $x(t)$  from  $x_0$ . The invariance of the magnetic induction equation to a change in the sign of the magnetic field implies that  $v(x)$  is an odd function of  $x$ , requiring  $v(x)$  to vanish at  $x = 0$ . A simple nonlinear extension of (3) is

$$v_{nl}(x) = -\frac{\gamma x}{x_0}(x - x_0) \quad \text{for } x \geq 0 \quad (4)$$

where the expected symmetry is obtained by taking  $v_{nl}(-x) = -v_{nl}(x)$ . In this study, calculations for variations in the trend are based mainly on the linear model, so the details of the nonlinear extension are not crucial. However, we do calculate the variability of trends using long simulations of the nonlinear model. Computing trends from these simulations include the influences of polarity reversals, which are absent from the theory based on the linear drift model.

Model parameters for the stochastic model are recovered from a wide variety of paleomagnetic observations using a Bayesian feature-based inversion (Morzfeld & Buffett, 2019). The input data sets includes 2-Myr records of paleointensity from the SINT-2000 (Valet et al., 2005) and PADM2M (Ziegler et al., 2011) models, as well as high-resolution records from the CALS10k.2 model (Constable et al., 2016) and the average reversal rate from the last 10 Myr (Ogg, 2012). Figure 2 shows the nonlinear drift term and the constant noise term from the inversion. A double potential well,  $U(x)$ , and a steady-state probability density function,  $P(x)$ , are defined using the drift and noise terms (see Figure 2b). Several other quantities were recovered in the inversion to characterize the correlation time of the noise source (see Table 1).

Departures from a Wiener process are expected at short time intervals due to correlations in the physical processes that generate fluctuations in the dipole field. We resolve this complication by considering exponentially correlated noise (Hänggi & Jung, 1995). The correlation time of the noise is  $\tau_\alpha = \alpha^{-1}$ , where  $\alpha$  is a parameter recovered in the inversion. A second correlation time is introduced to account for the gradual acquisition of magnetization in marine sediments (Roberts & Winklhofer, 2004). These

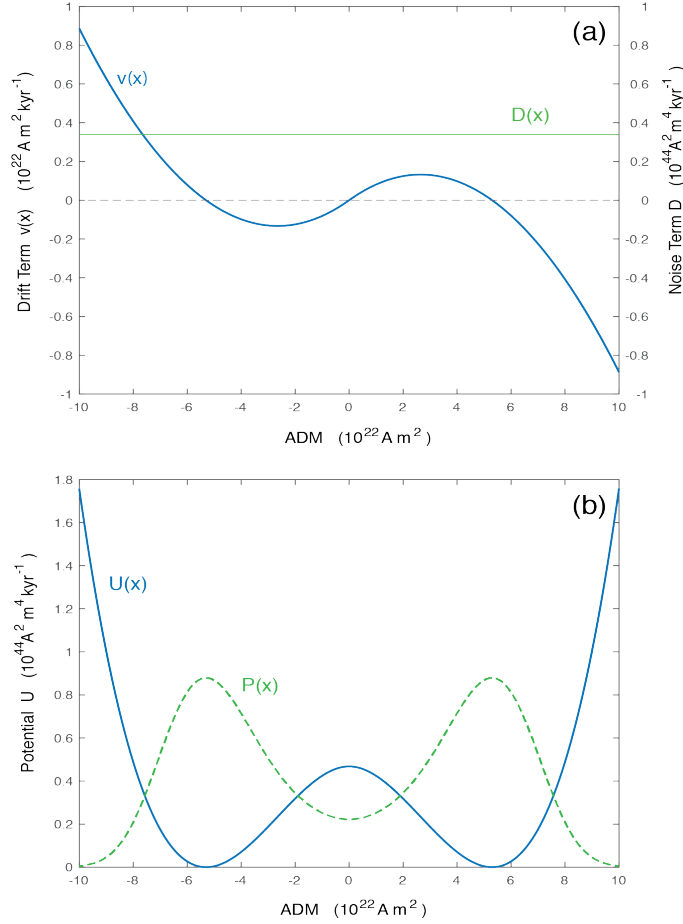


**Figure 2.** (a) Nonlinear drift (blue) and noise (green) terms for the stochastic model. (b) A double potential well  $U(x)$  is defined by integrating  $-v(x)$  with respect to  $x$ . The steady-state probability distribution of  $x$  is proportional to  $P(x) \sim \exp(-U/D)$ .

affects are approximated by applying a filter to the stochastic model (Buffett & Puranam, 2017), effectively introducing a second correlation time related to the sedimentary record. It is important to note that this second correlation time has no physical connection to processes that generate the magnetic field. Instead, it is intended to reflect the acquisition of magnetization in marine sediments. We only use the second correlation time (denoted by  $\tau_{sed}$ ) when making comparisons between the stochastic model and the marine record of relative paleointensity.

### 3 Variability of the Trend

An analytical solution of the stochastic differential equation in (2) is possible when the drift term is linear and the noise term is constant. The general solution for the deviation from the mean,  $\epsilon(t) = x(t) - x_0$ , is (Risken, 1989)

$$\epsilon(t) = \epsilon(t_0)e^{-\gamma(t-t_0)} + \sqrt{2D} \int_{t_0}^t e^{-\gamma(t-s)} dW_s \quad (5)$$

where  $\epsilon(t_0)$  defines the initial condition at  $t_0$ . All memory of the initial condition is lost at large times, so we can adopt an initial condition at  $t_0 = -\infty$  and write the solution for  $\epsilon(t)$  solely in terms of a sequence of random increments,  $dW_s$ . The trend of  $\epsilon(t)$  over

a time window  $w$  can be written as (Kenney & Keeping, 1962)

$$b = \frac{\text{Cov}(t, \epsilon)}{\text{Var}(t)} \quad (6)$$

where  $\text{Cov}(t, \epsilon)$  is the covariance between  $t$  and  $\epsilon$ , and  $\text{Var}(t)$  is the variance of  $t$ . Choosing a time window between  $-w/2$  and  $w/2$  means that the expected value of  $t$  vanishes. The resulting expression for  $\text{Var}(t)$  reduces to

$$\text{Var}(t) = \frac{1}{w} \int_{-w/2}^{w/2} t^2 dt = \frac{w^2}{12}. \quad (7)$$

The covariance between  $t$  and  $\epsilon(t)$  is calculated using the analytical solution in (5), and the variance of the trend is given by

$$\sigma_b^2 \equiv \text{Var}(b) = E(b^2) - E(b)^2. \quad (8)$$

Nijse et al. (2019) derived a closed-form expression for  $\sigma_b$  in the context of a related problem in climate science. We defer the details to a supplement, and simply state the general form of the standard deviation

$$\sigma_b = \sqrt{24\gamma D f(\gamma w)} \quad (9)$$

where  $f$  is a known function of  $\gamma w$  (or, equivalently  $w/\tau_\gamma$ ). We also derive a useful small- $w$  approximation for  $\sigma_b$

$$\sigma_b = \sqrt{\frac{2D}{w}} \quad (10)$$

which is independent of  $\gamma$ . It is important to note that (10) is valid when  $w$  is short relative to  $\tau_\gamma$  but long relative to the correlation time of the noise term.

Figure 3 shows the theoretical prediction for  $\sigma_b$  from (9), as well as the small- $w$  approximation in (10). We also show the standard deviation of the trend from a long simulation of the stochastic model with the nonlinear drift term. This simulation includes polarity reversals, which are absent from the theory. Including reversals appears to cause a small increase in  $\sigma_b$  relative to the theory at large  $w$ . We also show the standard deviation of the trends from the higher resolution CALS10k.2 model, as well as the longer time-scale/lower resolution SINT-2000 and PADM2M models. There is general agreement between the theory and the paleomagnetic models, although the variability of the lower resolution models falls below the prediction when the window length is less than 20 kyr. This discrepancy may be due to gradual acquisition of magnetization in marine sediments (Roberts & Winkholfer, 2004) or the model regularization (Ziegler et al., 2011). The resulting smoothing should reduce the variability of the observed trends at short window lengths.

The historical trend for a 170-year window lies above the theoretical prediction. However, it is well within the allowable range of the stochastic model. Fluctuations in the trend follow a normal distribution (see Supplement), so the predicted standard deviation,  $\sigma_b = 2.18 \times 10^{22} \text{ A m}^2$ , for a window of  $w = 170$  years means that the historical trend corresponds to a  $2.1\sigma_b$  event. The chances of the stochastic model producing a (negative) trend at or in excess of the historical trend is about 1.8%. Allowing for the influence of correlated noise would likely lower the probability of the historical trend (see Section 4), but it remains a plausible outcome of the stochastic model. Extending the historical trend for another 1.66 kyr is much less likely. The predicted standard deviation is  $\sigma_b = 0.68 \times 10^{22} \text{ A m}^2$  at  $w = 1.66$  kyr, so the proposed extension of the historical trend would correspond to a  $6.7\sigma_b$  event. The probability of this event is vanishingly small. We can safely conclude that the historical trend cannot be used as the basis for predicting the next geomagnetic reversal.

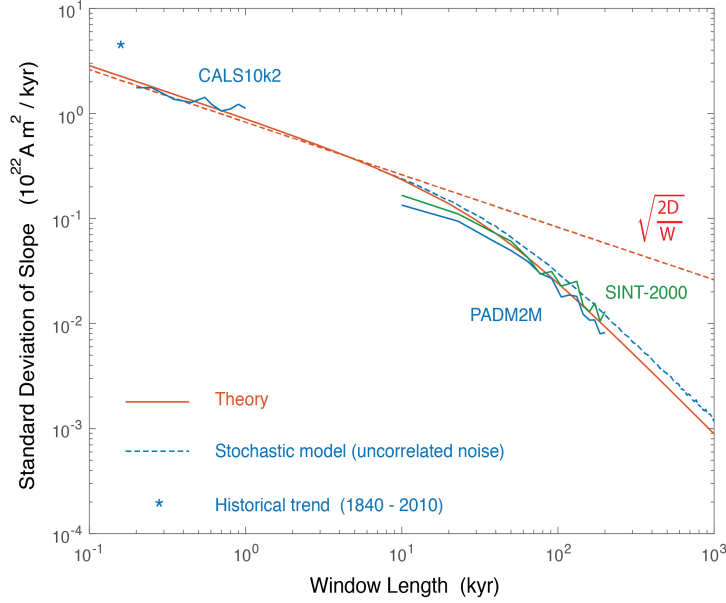


**Figure 3.** Theoretical predictions for the standard deviation of the trend (red) and a useful approximation at small  $w$  (red dash). Estimates from several paleomagnetic models (CALS10k2, PADM2M and SINT-2000) are shown for comparison. The historical trend over a 170-year window is also shown. A long realization of the stochastic model with the nonlinear drift term produces larger variability than the theory at large  $w$ , possibly due to the effects of polarity reversals. Much closer agreement between the theory and the simulation occurs at short  $w$ .

#### 4 Influence of Correlated Noise

The stochastic model in (2) is driven by random increments,  $dW_t$ , which are assumed to be statistically independent. This assumption is reasonable when the time step,  $\Delta t$ , is large, but it becomes questionable when  $\Delta t$  approaches the correlation time of the noise model. Morzfeld and Buffett (2019) recovered a correlation time of  $\tau_\alpha = 120$  years from the high-resolution CALS10k.2 model. This time interval is comparable to the length of the historical record, so our assessment of the historical record using the stochastic model may require an explicit treatment of correlated noise. This is implemented in the stochastic model by replacing  $dW_t$  with an exponentially correlated noise source. The required modifications are fairly standard and the details can be found in Morzfeld and Buffett (2019).

Figure 4 shows the standard deviation of the trend computed from a simulation of the stochastic model with correlated noise. The influence of correlation lowers the standard deviation of the trend at short window lengths. Departures from the theoretical value of  $\sigma_b$  first become evident when  $w$  is roughly a factor of ten larger than the correlation time. For a correlation time of 120 years we see departures below  $w = 1$  kyr, and these changes become larger with further reductions in  $w$ . The standard deviation in the simulation at  $w = 170$  year decreases to  $\sigma_b = 1.45 \times 10^{22} \text{ A m}^2$ , which means that the historical record now corresponds to a  $3.1\sigma_b$  event. This change lowers the probability of the historical trend to about 0.1%. Accounting for uncertainties in  $D$  and  $\tau_\alpha$  allow a modest increase in the probability of the historical trend. For example, a one-sigma change in  $D$  and  $\tau_\alpha$  can increase the standard deviation to  $\sigma_b = 1.56 \times 10^{22} \text{ A}^2 \text{ m}$ , which makes the historical rate a  $2.9\sigma_b$  event (corresponding to a 0.2% probability). Attributing  $\tau_\alpha$  solely to physical processes in the core appears to make the historical trend



unusual. On the other hand, it is possible that  $\tau_\alpha$  includes affects associated with the measurements or regularization in the model construction. Reducing the correlation time to reflect only physical processes would shift  $\sigma_b$  at  $w = 170$  year toward the theoretical prediction, making the historical record more likely. This change would also improve the agreement between the correlated stochastic model and the estimates of  $\sigma_b$  from CALS10k.2. (The previous inference of  $\tau_\alpha$  from CALS10k.2 was based on the power spectrum of dipole fluctuations).

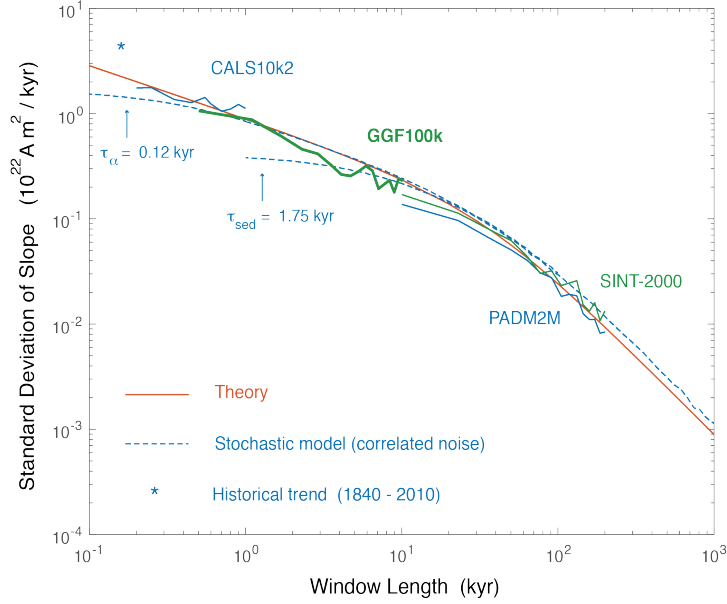


**Figure 4.** Standard deviation of the trend from simulations with correlated noise (blue dash). The correlation time  $\tau_\alpha$  is intended to represent processes in Earth’s core, while  $\tau_{sed}$  reflects the smoothing in marine sediments. The theory (red) and trends from four paleomagnetic models are shown for comparison. Model GGF100k (bold green) was not used in the construction of the stochastic model.

A second simulation of the stochastic model is computed with a correlation time of  $\tau_{sed} = 1.75$  kyr to mimic the effects of smoothing in marine sedimentary records (see Figure 4). The standard deviation of the trend in the simulation shows similarities with the trends computed from PADM2M and SINT-2000. Both the simulation and paleomagnetic models are consistent with the theory at large  $w$ , but there is a gradual departure at smaller  $w$ . The nature of this departure is qualitatively similar in the simulation and paleomagnetic models, although there are quantitative differences in the overall amplitude. One way to reconcile the stochastic model with SINT-2000 and PADM2M is to increase slightly the value of  $\tau_{sed}$ . This modification would have two consequences. First, it would cause departures from the theory at longer  $w$ , consistent with estimates from the paleomagnetic models. Second, it would produce a lower  $\sigma_b$  in the vicinity of  $w = 10$  kyr. The sensitivity of  $\sigma_b$  to  $\tau_{sed}$  may offer a new diagnostic to characterize the acquisition of magnetization in marine records.

Figure 4 also shows the results from an intermediate-resolution paleomagnetic model, known as GGF100k (Panovska et al., 2019). This model is constructed from lake and marine sediments, as well as volcanic and archeomagnetic observations from the past 100 kyr. The paleomagnetic field is resolved into spherical harmonic components (like CALS10k.2), but it has less temporal resolution. Variations in the computed trends fill the gap in win-

dow length between CALS10k.2 and the lower resolution models (SINT-2000 and PADM2M). The computed standard deviation agrees well with theory, particular at shorter window lengths where a larger number of estimates for  $b$  give more reliable statistics. The trends from GGF100k are notable because this model was not used in the inversion for the parameters of the stochastic model.

## 5 Implications for the Next Polarity Reversal

Estimates for  $\sigma_b$  as a function of  $w$  can be used to make inferences about the timing of the next polarity reversal. We apply the theory with uncorrelated noise and assume the current dipole moment,  $x(t_c)$ , is brought to zero over a time interval  $w$ . The required trend is  $b = -x(t_c)/w$ . We can now use the standard deviation,  $\sigma_b$ , at this value of  $w$  to assess whether the required trend is likely. Alternatively, we can specify the likelihood of the trend and evaluate the window length required to produce this probability. For example, there is a 2% chance of sustaining a negative trend  $b \leq -2.05\sigma_b$ . If we set the required trend equal to  $-2.05\sigma_b$ , then we require

$$\frac{x(t_c)}{w} \approx 2.05\sqrt{\frac{2D}{w}} \quad (11)$$

using the small- $w$  approximation in (10). Solving for  $w$  gives

$$w = \frac{x(t_c)^2}{8.4D}. \quad (12)$$

Taking  $x(t_c) = 7.6 \times 10^{22}$  A m<sup>2</sup> gives  $w = 20.2$  kyr. In other words, there is roughly a 2% chance that the axial dipole moment will decline to zero in the next 20 kyr or less.

A remarkably similar prediction was made using a solution of the backward Fokker-Planck equation (Buffett & Davis, 2018). This agreement may be surprising at first glance because the solution in (12) has the form of a purely diffusive process with no dependence on the drift term (e.g. Shcherbakov & Fabian, 2012). While the drift term appears in the backward Fokker-Planck equation, its contribution to the predicted probability is small when the solution is evolved over a short time interval. This result is consistent with expectations that the dipole moment is driven mainly by the noise term over timescales less than  $\tau_\gamma$ . Indeed, we find good agreement between the small- $w$  approximation in (10) and the predictions of the full theory for  $\sigma_b$  when  $w < \tau_\gamma$  (see Figure 3). The unexpected outcome is that (12) gives good agreement with the more rigorous treatment even when  $w \sim \tau_\gamma$ .

An alternative statistical description of polarity reversals is based on a model for a Poisson point process (e.g. Cox, 1968). In this case the probability of a reversal occurring within a time interval  $w$  is

$$P(t < w) = 1 - e^{-rw} \quad (13)$$

where  $r = 4.4$  Myr<sup>-1</sup> is the mean reversal rate from the last 5 Myr (Ogg, 2012). Considering a time interval of  $w = 20$  kyr gives a probability of 8.4%, which is about four times larger than the probability predicted using (12). Reducing the time interval to  $w = 2$  kyr gives a probability of 0.88%. The same probability ( $P = 0.88\%$ ) describes the chances of sustaining a negative trend  $b < -3.13\sigma_b$ . Using this updated value for the trend in (12) gives  $w = 8.7$  kyr, compared to  $w = 2$  kyr for a Poisson process. Alternatively, we might fix the window length at  $w = 2$  kyr, and determine the initial value for  $x(t_c)$  needed to reproduce the prediction of the Poisson process. We require  $x(t_c) = 3.65 \times 10^{22}$  A m<sup>2</sup>, indicating that the amplitude of the initial dipole moment is important for predicting the probability of a reversal using the stochastic model.

## 6 Conclusions

Historical trends in the dipole moment are sometimes used to speculate about a polarity reversal in the next several thousand years. We argue against this extrapolation by showing that the historical trend should be interpreted as a short-term fluctuation. A simple statistical analysis of the CALS10k.2 model suggests that the chances of sustaining the historical trend over a 200-year interval is about 0.6%. Increasing the duration of this trend to 500 years lowers the probability to about 0.1%. We develop a quantitative model to assess the variability of trends in the dipole moment over arbitrary window lengths. The model is based on a stochastic differential equation with parameters recovered from a variety of paleomagnetic observations. We show that the model reproduces the statistics of trends from the CALS10k.2 model (Constable et al., 2016). It also reproduces the statistics of trends from the PADM2M (Ziegler et al., 2011), SINT-2000 (Valet et al., 2005) and GGF100k (Panovska et al., 2019), provided the window length is long compared with the time required for sediments to acquire magnetization. Applying the model to the historical record shows that the probability of sustaining the current trend for next several thousand years is virtually zero. Instead, we compute the trend needed to reduce the axial dipole moment to zero with a specified probability. We find that dipole moment could vanish in the next 20 kyr with a probability of 2%.

## Acknowledgments

This work is supported a grant (EAR-1644644) from National Science Foundation to B.B. and by Posdoctoral Fellowship (EAR-1725798) from the National Science Foundation to M.S.A. Paleomagnetic models used in this study were obtained from <https://earthref.org>. The stochastic models are available at <https://earthref.org/ERDA/2413>. We thank Matti Morzfeld and anonymous reviewer for thoughtful comments. We also thank Tushar Mittal for bring the study of Nijse et al. (2019) to our attention.

## References

- Buffett, B., & Davis, W. (2018). A probabilistic assessment of the next geomagnetic polarity reversal. *Geophysical Research Letters*, *45*, 1845-1850. doi: 10.1002/2018GL077061
- Buffett, B., King, E., & Matsui, H. (2014). A physical interpretation of stochastic models for fluctuations in the earth's dipole field. *Geophysical Journal International*, *198*(1), 597-608.
- Buffett, B., & Puranam, A. (2017). Constructing stochastic models for dipole fluctuations from paleomagnetic observations. *Physics of Earth Planetary Interiors*, *272*, 68-77. doi: 10.1016/j.pepi.2017.09.001
- Constable, C. (2007). Dipole moment variation. In D. Gubbins & E. Herrero-Bervera (Eds.), *Encyclopedia of geomagnetism and paleomagnetism* (p. 159-161). Springer.
- Constable, C., & Korte, M. (2006). Is earth's magnetic field reversing? *Earth and Planetary Science Letters*, *246*, 1-16. doi: 10.1016/j.epsl.2006.03.038
- Constable, C., Korte, M., & Panovska, S. (2016). Persistent high paleosecular variations in the southern hemisphere for at least 10000 years. *Earth and Planetary Science Letters*, *453*, 78-86. doi: 10.1016/j.epsl.2016.08.015
- Cox, A. (1968). Lengths of geomagnetic polarity intervals. *Journal of Geophysical Research*, *73*, 3247-3260. doi: 10.1029/JB073i010p03247
- De Santis, A., Qamili, E., & Wu, L. (2013). Toward a possible next geomagnetic transition? *Natural Hazards and Earth System Science*, *13*, 3395-3403. doi: 10.5191/nhess-13-3395-2013
- Gillet, N., Jault, D., Finlay, C., & Olsen, N. (2013). Stochastic modeling of the earth's magnetic field: Inversion for covariances over the observatory era. *Geochemistry, Geophysics, Geosystems*, *14*, 766-786. doi: 10.1002/ggge.20041

- Hänggi, P., & Jung, P. (1995). Colored noise in dynamical systems. *Advances in chemical physics*, 89, 239–326.
- Hulot, G., Eymin, C., Langlais, B., Manda, M., & Olsen, N. (2002). Small-scale structure of the geodynamo inferred from oersted and magsat satellite data. *Nature*, 416, 620–623. doi: 10.1016/j.pepi.2013.05.005
- Kenney, J. F., & Keeping, E. (1962). Linear regression and correlation. *Mathematics of statistics*, 1, 252–285.
- Kloeden, P. E., & Platen, E. (2013). *Numerical solution of stochastic differential equations* (Vol. 23). Springer Science & Business Media.
- Laj, C., & Kissel, C. (2015). An impending geomagnetic transition? Hints from the past. *Frontiers in Earth Science*, 3, 1–10. doi: 10.3389/feart.20015.00061
- Morzfeld, M., & Buffett, B. (2019). A comprehensive model for the kyr and myr timescales of earth’s axial magnetic dipole field. *Nonlinear Processes in Geophysics*, 26, 123–142. doi: 10.5194/npg-26-123-2019
- Morzfeld, M., Fournier, A., & Hulot, G. (2017). Coarse predictions of dipole reversals by low-dimensional modeling and data assimilation. *Physics of Earth and Planetary Interiors*, 262, 8–27. doi: 10.1016/j.pepi.2016.10.007
- Nijse, F., Cox, P., Huntingford, C., & Williamson, M. (2019). Decadal global temperature variability increases strongly with climate sensitivity. *Nature Climate Change*, 9, 598–601. doi: 10.1038/s41559-019-0527-4
- Ogg, J. G. (2012). Geomagnetic polarity time scale. In F. M. Gradstein (Ed.), *The geologic time scale 2012* (p. 85–113). Elsevier Science.
- Panovska, S., Constable, C. G., & Korte, M. (2019). Extending global continuous geomagnetic field reconstructions on timescales beyond human civilization. *Geochemistry, Geophysics, Geosystems*, 19, 4757–4772. doi: 10.1029/2018GC007966
- Poletti, W., Biggin, A., Trindade, R., Hartmann, G., & Terra-Nova, F. (2018). Continuous millennial decrease of the earth’s geomagnetic axial dipole. *Physics of the Earth and Planetary Interiors*, 274, 72–86. doi: 10.1016/j.pepi.2017.11.005
- Risken, H. (1989). *The Fokker-Planck equation*. New York: Springer.
- Roberts, A. P., & Winklhofer, M. (2004). Why are geomagnetic excursions not always recorded in sediments? Constraints from post-deformation remanent magnetization lock-in modeling. *Earth and Planetary Science Letters*, 227, 345–359. doi: 10.1016/j.epsl.2004.07.040
- Shcherbakov, V., & Fabian, K. (2012). The geodynamo as a random walker: A view on reversal statistics. *Journal of Geophysical Research*, B, 117, B03101. doi: 10.1029/2001JB008931
- Valet, J. P., Meynadier, L., & Guyodo, Y. (2005). Geomagnetic dipole strength and reversal rate over the past two million years. *Nature*, 435, 802–805. doi: 10.1038/nature03674
- Van Kampen, N. (2007). *Stochastic processes in physics and chemistry*. Amsterdam: Elsevier.
- Ziegler, L. B., Constable, C. G., Johnson, C. L., & Tauxe, L. (2011). PADM2M: a penalized maximum likelihood model for the 0–2 Ma paleomagnetic axial dipole moment. *Geophysical Journal International*, 184, 1069–1089. doi: 10.1111/j.1365-246X.2010.04905.x